



Synthesis, characterization, and antiproliferative activities of new transition metal complexes with 3-((4-fluoro-2-hydroxybenzylidene)amino)-2-thioxoimidazolidin-4-one

Lamia A. Ismail^{1,*}, Eman M. Hassan¹, A.A.El-Bindary², Reda F.M. Elshaarawy^{3,4}, R. Zakaria¹

¹ Department of Chemistry, Faculty of Science, Port Said University, 42526 Port Said, Egypt

² Chemistry Department, Faculty of Science, Damietta University, Damietta, 34517, Egypt

³ Department of Chemistry, Faculty of Science, Suez University, 43533 Suez, Egypt.

⁴ Institut für Anorganische Chemie und Strukturchemie, Heinrich-Heine Universität Düsseldorf, Düsseldorf, Germany.

*Corresponding author: lamia_zayat@yahoo.com

ABSTRACT

The effective synthesis of a novel Schiff base ligand, namely ((fluorosalicylidene)amino) thiohydantoin (FSATH), and its corresponding coordination compounds (M(II)-FSATH; M = Mn, Co, Cu, Zn), has been achieved. Several micro-analytical, spectral (FTIR, UV-Vis, NMR, and EI-MS), magnetic, and thermal techniques were employed to ascertain the stoichiometry, complexation styles, geometry, and thermal stability of the new coordination compounds (M-FSATH). The findings of these measurements demonstrated that the FSATH ligand coordinates through the azomethine nitrogen, phenolic oxygen, and thiocarbonyl sulfur atoms to the metal ion. All coordination compounds examined against human breast carcinoma cells (MCF-7) showed increased cytotoxicity relative to the parent ligands, as determined by comparative *in-vitro* anticancer studies. Cu-FSATH demonstrates significant cytotoxicity against MCF-7, making it a highly promising alternative to conventional chemotherapeutic agents.

Key Words:

(Fluorosalicylidene)-aminothiohydantoin, Metal(II) coordination compounds, Spectroscopic study, Cytotoxicity.

1- INTRODUCTION

The concept of pharmacophore hybridization plays a crucial role in modern drug development, offering a promising approach to optimizing the pharmacological properties of potential therapeutic

agents [1]. This approach enables drug designers to exploit the synergistic effects of multiple pharmacophores, thereby improving the overall therapeutic profile of the drug candidate. Pharmacophore hybridization has been successfully employed in the development of several drugs, such as HIV protease inhibitors, antimalarial agents, and anticancer drugs [2]. By combining the pharmacophoric elements from different lead compounds, researchers can design and synthesize hybrid molecules that exhibit improved potency, selectivity, and pharmacokinetic properties. This strategy offers a valuable tool in the quest for novel and more effective therapeutic agents.

Thiohydantoin is a class of organic compounds that have attracted significant attention due to their diverse biological activities. These compounds are characterized by a thiohydantoin ring, an imidazolidine ring attached to thiocarbonyl and carbonyl groups. The presence of this ring imparts specific chemical and biological properties to these compounds, making them versatile and valuable in various biological applications. Thiohydantoin has been found to exhibit a wide range of biological activities, including antimicrobial, anti-inflammatory, anticonvulsant, and anticancer properties. These characteristics make them attractive candidates for the development of novel drugs targeting various diseases. For instance, thiohydantoin has shown potential in the treatment of cancer by inhibiting key enzymes and pathways involved in tumor growth and metastasis. Additionally, the modification of thiohydantoin has led to the discovery of compounds with enhanced bioavailability and improved pharmacokinetic profiles. The versatility of thiohydantoin allows for structural modifications, facilitating the development of compounds with specific drug-like properties. Furthermore, the synthesis of thiohydantoin can be achieved through efficient and cost-effective methods, making them even more appealing for drug development [3-7]. New 3,5-disubstituted-2-thiohydantoin 5a-c were developed and produced by Elbadawi et al. (2022). Thiohydantoin derivatives have shown promising antiproliferative action, with IC_{50} ranges of 1.980-19.089 μ M for prostate (PC-3) and 1.619-16.976 μ M for breast (MCF-7) cancer cell lines [8]. Of particular note, enzalutamide (**Figure 1**), which is based on thiohydantoin, has been licensed for use in humans as an androgen receptor antagonist medication [3]. Further research and exploration of thiohydantoin and their derivatives hold great promise for the development of novel drugs and treatments in the future.

Meanwhile, transition metal coordination compounds with thiohydantoin have gained significant attention in the field of biological applications due to their diverse range of properties and mechanisms. The biological activities of these coordination compounds are attributed to their ability to interact with biomolecules such as DNA, proteins, and enzymes. For example, transition metal coordination compounds with thiohydantoin have been found to exhibit DNA-binding properties, leading to DNA damage and inhibition of DNA replication. Additionally, these coordination compounds have been shown to interact with enzymes, inhibiting their activity and disrupting cellular processes. Furthermore, the coordination of thiohydantoin with transition metals can enhance their solubility and stability, making them more effective in biological systems. Overall, the exploration of the biological applications and mechanisms of transition metal coordination compounds with thiohydantoin holds great promise for the development of novel therapeutic agents with improved efficacy and specificity [5-7].

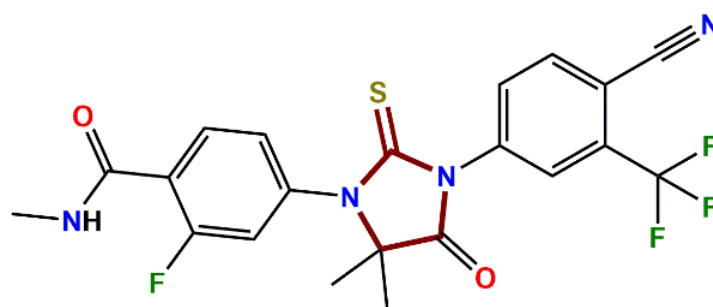


Figure 1: Chemical structure of a clinically approved thiohydantoin-based drug (enzalutamide).

Due to these astounding facts, as well as our continuous efforts to develop and explore new chemotherapeutic candidates [8-10], the current work aims to develop new thiohydantoin-based ligands and their M(II) coordination compounds (M = Mn, Co, Cu, Zn) for use in chemotherapy targeting breast cancer by employing a variety of drug design methodologies. Furthermore, a range of biochemical and biological investigations will be carried out in the course of this work to clarify the possible molecular mechanism of interaction between these chemicals and cancer cells.

2- Experimental

2.1. Overveiw

We used all commercially available substrates and reagents without any additional purification. Distillation and conventional drying methods were used to purify the solvents before they were used.

BÜCHI melting point B-540 equipment was used to measure the melting points (mp); all measurements were made in open glass capillaries and are uncorrected. The Perkin–Elmer 263 elemental analyzer was used to conduct elemental analysis for CHNS. Using a BRUKER Tensor-37 FTIR spectrophotometer, Fourier transform infrared (FTIR) spectra were captured as KBr discs in the 400–4000 cm^{-1} range. The UV-Vis spectra were obtained at 25 °C in ethanol solution (10^{-3} M) using a Shimadzu UV-2450 spectrophotometer and quartz cuvettes of a path length of 1 cm. NMR spectra were acquired using a Bruker Avance DRX200 or DRX500 spectrometer. The signals' multiplicities were given as singlet (s), doublet (d), triplet (t), quartet (q), or multiplet (m). Electro-impact mass spectra (EI-MS) were recorded using Shimadzu and the GCMS 5988-A HP spectrometer at an ionizing voltage of 70 eV.

1.1. Synthesis of 4-fluorosalicylaldehyde thiosemicarbazone (FSTSC)

A solution was prepared by dissolving 1.4 g (10.0 mmol) of 4-fluorosalicylaldehyde and 0.91 g (10.97 mmol) of thiosemicarbazide in 10 mL of distilled water, along with a catalytic amount of acetic acid. The resulting mixture was then dissolved in 30 mL of ethanol and heated gently with stirring until a clear solution was obtained. After 4 h of refluxing, the solvent was partially removed and the mixture was subsequently cooled to ambient temperature. The precipitate was filtered, dried, and purified through recrystallization using hot ethanol, resulting in the desired pure thiosemicarbazone (FSTSC). It was obtained as white crystals with a 76% yield and mp of 177–179 °C. FTIR (KBr) cm^{-1} : 3429 and 3301 (s, sh, ν_{NH_2}), 3229 (m, sh), 1631 (s, sh), 1561 (s, sh), 1273 (m, sh). ^1H NMR (DMSO- d_6 , 200 MHz) δ 11.41 (s, 1H), 10.40 (s, 1H), 8.36 (s, 1H), 8.09 (s, br, 2H), 7.49 (dd, $J = 1.9, 8.1$ Hz, 1H), 6.89–6.78 (m, 2H). ^{13}C NMR (DMSO- d_6 , 100 MHz) δ 177.98, 166.73, 162.12, 148.03, 132.46, 119.81, 112.25, 109.92. Anal. Calcd for $\text{C}_8\text{H}_8\text{FN}_3\text{OS}$ (M = 213.23 g/mol): C, 45.06; H, 3.78; N, 19.71; S, 15.04%. Found: C, 44.96; H, 3.88; N, 18.58; S, 14.97%.

1.2. Synthesis of 3-((4-fluoro-2-hydroxybenzylidene)amino)-2-thioxoimidazolidin-4-one

A homogenous mixture was prepared by combining 1.09 g (5.0 mmol) of FSTSC with 0.60 mL (5.0 mmol) of ethyl chloroacetate in 30 mL of dry ethanol containing 0.73 g (9.12 mmol) of anhydrous sodium acetate under vigorous stirring. After that, the mixture underwent reflux for 5 h with continuous stirring. TLC was employed to monitor the progression of the reaction. When the reaction was complete, the contents were cooled to room temperature and diluted using an ice-water mixture. The pure thiohydantoin ligand (FSATH) was obtained by separating the solid product, washing it with cold ethanol, drying it, and then recrystallizing it from hot ethanol. It was obtained as pale yellow crystals with a 78% yield and mp of 253–255 °C. FTIR (KBr) cm^{-1} : 3442 (m, br), 3318 (s, sh), 2981 (m, sh), 1716 (s, sh), 1640 (s, sh), 1539 (m, sh), 1488 and 1332 (m, sh), 1266 (s, sh), 1200 (m, sh), 1061, 973, 893 (m, sh), 782 (w, sh), 753 (w, sh). ^1H NMR (DMSO- d_6 , 300 MHz) δ 11.40 (s, 1H), 11.16 (s, 1H), 10.92 (s, 1H), 9.90 (s, 1H), 9.01 (s, 1H), 8.39–7.93 (m, 3H), 7.59–6.97 (m, 3H), 3.98 (s, 2H, s, 2H). ^{13}C NMR (DMSO- d_6 , 100 MHz) δ

178.07, 174.51, 165.24, 163.31, 159.12, 156.67, 139.99, 133.73, 132.63, 131.55, 131.06, 127.17, 120.82, 119.99, 118.91, 117.01, 116.48, 33.90. EI-MS: peak at $m/z = 253.25$ a.m.u. assigned to $[C_{10}H_8FN_3O_2S, M]^+$. Anal. Calcd for $C_{10}H_8FN_3O_2S$ ($M = 253.25$ g/mol): C, 47.43; H, 3.18; N, 16.59; S, 12.66%. Found: C, 47.28; H, 3.29; N, 16.48; S, 12.47%.

2.1. Synthesis of FSATH coordination compounds

The FSATH coordination compounds were prepared using the following general procedure: A 25-mL mixed solvent containing equal parts water and ethanol was prepared and used to dissolve a 1 mmol amount of a metal (II) salt ($MCl_2 \cdot xH_2O$; $CoCl_2 \cdot 2H_2O$, $CuCl_2 \cdot 2H_2O$, $MnCl_2 \cdot 4H_2O$, $ZnCl_2$). The metal salt solution was heated along with a 25 mL ethanolic solution containing FSATH (0.265 g, 1 mmol) and a small amount of NH_3/NH_4Cl buffer (pH 9.0). The content was refluxed for a duration of 2 hours. After that, at low pressure, some of the solvent was evaporated. Once the reaction mixture reached room temperature, the required compounds could be precipitated. The products were obtained through filtration and then subjected to a series of washing steps using water (three times with 5 mL), warm ethanol (three times with 5 mL), and diethyl ether (three times with 5 mL). Finally, the products were dried under a vacuum.

[Mn(FSATH)Cl(H₂O)₂].2H₂O (Mn-FSATH): Brown solid (65%). FTIR (KBr, cm^{-1}): 3430 (s, sh), 1715 (s, sh), 1620 (s, sh), 1541 (s, sh), 1470 (m, sh), 1339 (s, sh), 1273 (m, sh), 1179 (w, sh), 1145 (m, sh), 1069 (m, sh), 979 (w, sh), 849 (m, sh), 751 (m, sh), 621 (w, sh), 489 (s, sh), 407 (m, sh). EI-MS: m/z 396.65 ($C_{10}H_{13}ClFMnN_3O_5S, [M]^+$). Anal. Calcd. for $C_{10}H_{13}ClFMnN_3O_5S$ ($M = 396.68$ g/mol): C, 30.28; H, 3.30; N, 10.59; S, 8.08%. Found: C, 30.21; H, 3.33; N, 10.43; S, 7.89%.

[Co(FSATH)Cl(H₂O)₂].2H₂O (Co-FSATH): Purple solid (62%). FTIR (KBr, cm^{-1}): 3432 (s, sh), 1716 (s, sh), 1605 (s, sh), 1537 (s, sh), 1467 (m, sh), 1339 (s, sh), 1251 (m, sh), 1181 (w, sh), 1145 (m, sh), 1022 (m, sh), 980 (m, sh), 852 (m, sh), 788 (m, sh), 741 (w, sh), 621 (s, sh), 489 (s, sh), 409 (m, sh). EI-MS: m/z 400.65 ($C_{10}H_{13}ClCoFN_3O_5S, [M]^+$). Anal. Calcd. for $C_{10}H_{13}ClCoFN_3O_5S$ ($M = 400.67$ g/mol): C, 29.98; H, 3.27; N, 10.49; O, S, 8.00%. Found: C, 29.89; H, 3.34; N, 10.39; S, 7.91%.

[Cu(FSATH)Cl].2H₂O (Cu-FSATH): Reddish-brown solid (71%). FTIR (KBr, cm^{-1}): 3438 (s, sh), 3339 (s, sh), 1717 (s, sh), 1609 (s, sh), 1539 (s, sh), 1469 (m, sh), 1389 (m, sh), 1254 (s, sh), 1149 (m, sh), 1069 (w, sh), 989 (m, sh), 848 (m, sh), 749 (m, sh), 609 (m, sh), 522 (w, sh), 467 (m, sh), 449 (w, sh). EI-MS: m/z 387.25 ($C_{10}H_{11}ClCuFN_3O_4S, [M]^+$). Anal. Calcd. for $C_{10}H_{11}ClCuFN_3O_4S$ ($M = 387.27$ g/mol): C, 31.01; H, 2.86; N, 10.85; S, 8.28%; Found: C, 30.98; H, 2.89; N, 10.78; S, 8.21%.

[Zn(FSATH)Cl].H₂O (Zn-FSATH): Dirty-white solid (59%). FTIR (KBr, cm^{-1}): 3441 (s, br), 3338 (m, sh), 1715 (s, sh), 1615 (s, sh), 1439 (m, sh), 1339 (m, sh), 1258 (s, sh), 1147 (m, sh, ν_{C-S}), 1079 (m, sh), 985 (m, sh), 851 (m, sh), 801 (m, sh), 746 (m, sh), 608 (m, sh), 569 (w, sh), 517 (m, sh), 459 (m, sh). EI-MS: m/z 371.00 ($C_{10}H_9ClFN_3O_3SZn, [M]^+$). Anal. Calcd. for $C_{10}H_9ClFN_3O_3SZn$ ($M = 371.09$ g/mol): C, 32.37; H, 2.44; N, 11.32; S, 8.64%. Found: C, 32.29; H, 2.49; N, 11.27; S, 8.58%.

2.2. Anticancer assay

2.2.1. Cell cultivate

The breast cancer cell lines (MCF-7) were acquired from the American Type Cell Culture Collection (ATCC) in the USA. MCF-7 cells were grown in DMEM (Dulbecco's Modified Eagle's Medium) with 10% thermally-inactivated FBS fetal bovine serum), and antibiotics at concentrations of 100 units per milliliter (U/mL) of penicillin and 100 μ g/mL of streptomycin. Heracell VIOS carbon dioxide incubator was utilized to maintain the cells at a temperature of 37 °C within a controlled environment with a humidity level of 5% CO₂.

2.2.2. Anti-proliferative activity

The *in vitro* anticancer activity of the newly synthesized compounds was evaluated against MCF-7 cells using the MTT assay. In summary, cell lines were subjected to treatment on a 96-well plate with varying quantities of compounds, as well as positive and negative controls. The cell density in each well was 105 cells, and the plate used was a Falcon brand from New Jersey, USA. The doses of the compounds tested were 0.4, 1.6, 6.3, 25, 50, and 100 μM . The positive control used was Vinblastine (VBL) ($\text{C}_{46}\text{H}_{58}\text{N}_4\text{O}_9$, 810.99 g/mol), while the negative control was dimethyl sulfoxide (DMSO). The wells have been categorized into groups, with each sample containing three wells. Subsequently, the plate was subjected to incubation at a temperature of 37 $^\circ\text{C}$ and in an environment containing 5% carbon dioxide. Following a 48-hour incubation period, the cells in each well were subjected to fixation, washing, and staining using an MTT reagent (5 mg/mL in a 0.9% NaCl solution). Subsequently, the cells were re-incubated for an additional 4 hours. Upon the conclusion of the incubation period, the plate was retrieved from the incubator and the staining solution was carefully extracted. Subsequently, the formazan crystals that had formed were dissolved by adding acidified isopropanol (180 μL per well). This process was carried out at room temperature with continuous agitation using a MaxQ 2000 plate shaker. After that, we used a Stat FaxR 4200 plate reader to do a spectrophotometric analysis by measuring the absorbance of the plate at 570 nm. The IC_{50} value was derived by quantifying the molar concentration required to achieve a 50% reduction in cell viability. The surviving fractions were expressed using the values of mean \pm S.E.

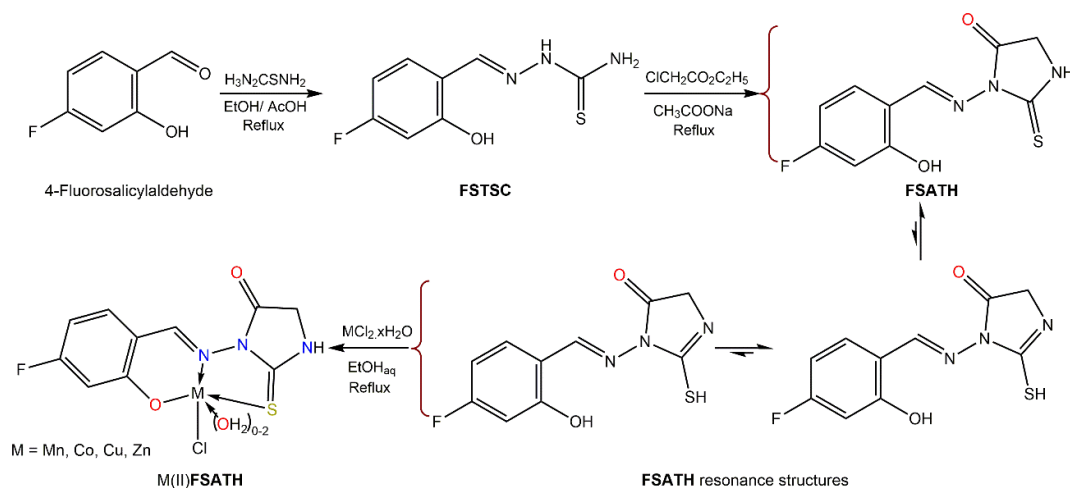
2.3. Statistical Analyses

The results and mathematical calculations for this study were conducted utilizing an independent student's t-test with the assistance of SPSS v17 and OriginPro 9.1 32. The findings were reported in terms of mean \pm standard median error, and statistical significance was determined at a threshold of $P < 0.05$.

3. RESULTS AND DISCUSSION

3.1. Synthesis chemistry

The preparation of the (fluorosalicylidene)-aminothiohydantoin ligand (FSATH) involved two sequential processes, as illustrated in **Scheme 1**, using 4-fluorosalicylaldehyde as the starting substrate. To obtain the equivalent fluorosalicylaldehyde thiosemicarbazone (FSTSC), a condensation reaction between fluorosalicylaldehyde and thiosemicarbazide in a catalytic acid medium is first performed. The thiosemicarbazone (FSTSC) was converted to FSATH via a cyclocondensation reaction between FSTSC and ethyl chloroacetate in the presence of $\text{CH}_3\text{COONa}_{(\text{anhydrous})}$ as a catalyst, which was carried out at reflux. The synthesis of Mn(II), Co(II) Cu(II), and Zn(II) coordination compounds of the FSATH ligand (M-FSATH) was carried out through the refluxing of solutions containing deprotonated FSATH with metal(II) chlorides in an ethanol-water mixed solvent (**Scheme 1**). The ATHSB was pre-deprotonated utilizing an ammonium buffer solution with a pH of 9.0. Regrettably, all endeavors to produce singular crystals of the M-FSATH coordination compounds suitable for X-ray analysis proved unsuccessful. Consequently, the postulated structures of the newly formed coordination compounds were derived from elemental (CHNS) analysis, as well as spectrum analyses utilizing techniques such as FTIR, UV-Vis, and EI-MS. Additionally, magnetic measurements were employed in the determination of these structures.



Scheme 1: Stepwise preparation of (fluorosalicylidene)-aminothiohydantoin ligand (FSATH) and its metal coordination compounds.

3.2. Structural characterization

The newly synthesized thiohydantoin derivatives, including both the parent ligand (FSATH) and its coordination compounds (M-FSATH) were acquired in favorable yields. The compounds were subjected to elemental (CHNS), spectroscopic, magnetic, and thermal investigations in order to investigate their structural formulas as well as thermal stability.

3.2.1. Elemental analyses and mass spectrometry

The findings of micro-analytical analysis (carbon, hydrogen, nitrogen, and sulfur percentages) for both the free ligand and its coordination compounds align completely with the proposed molecular formula for these compounds. Please refer to the experimental section for further details.

Meanwhile, molecular ion peaks ($[\text{M}]^{+\bullet}$) may be seen in the EI-MS (electron impact mass spectra) of all the parent ligand (see **Figure 2**) and its coordination compounds. The success of the synthesis can be verified by this finding.

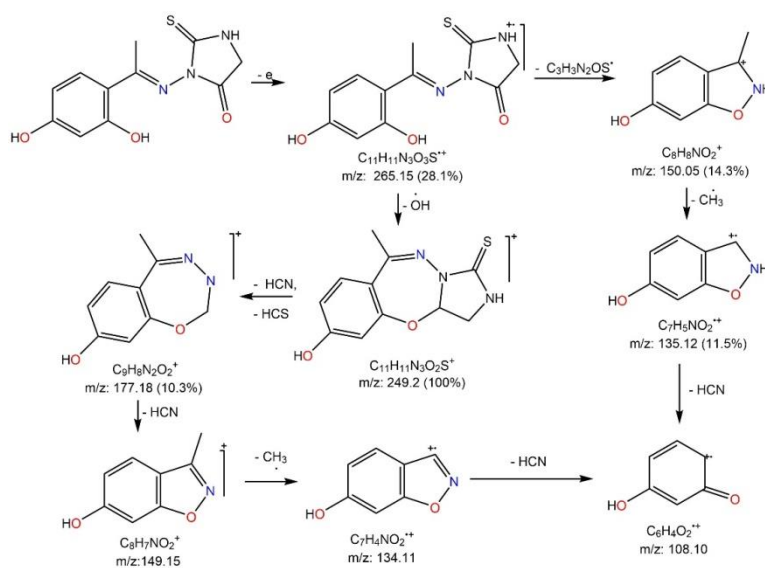


Figure 2: Proposed mass fragmentation pattern of the parent (fluorosalicylidene)-aminothiohydantoin ligand (FSATH) ligand.

3.2.2. Fourier transform infrared spectroscopy (FTIR)

FTIR spectroscopy is commonly employed as an initial and informative tool to verify the effective creation of novel compounds and investigate the binding modes present within them [9]. The analysis of the FTIR spectrum of the free FSATH ligand (**Figure 3** and **Table 1**) provides valuable insights into its molecular structure and functional groups. The presence of characteristic peaks in the spectrum, including the vibrations of the thioamide N–H, carbonyl (C=O), thiocarbonyl (C=S), asymmetric thioamide N–C=S, and symmetric thioamide N–C=S, which appears at around 3318, 1716, 1488, 1332, 1152, and 753 cm^{-1} , respectively [6,7] These peaks indicate the presence of the thiohydantoin ring, confirming its successful formation. Noteworthy, the absence of an infrared peak at approximately 2500 cm^{-1} in the FSATH spectrum indicates the absence of the $\nu_{\text{(S-H)}}$ stretch, confirming that the thiol form does not contribute to the molecular structure of FSATH. This suggests that the new ligand is mostly found in the thione form. Additionally, the emergence of IR peaks at around 3442, 1640, and 1266 cm^{-1} which are characteristic of phenol and imine functional groups confirms the formation of the Schiff base ligand [6,7].

On the other hand, the FTIR spectra of the M-FSATH coordination compounds show several intriguing characteristics. By studying the spectral peaks and their corresponding intensities, we can accurately determine the coordination mode of the metal ion and the ligand, as well as any potential changes that occur upon complexation. As an illustration, the removal of FSATH's band unique for the phenolic O-H group (3442 cm^{-1}) is proof that the phenolic OH group has been deprotonated and that the aryl-O is involved in the chelation of metal ions, along with a shift of the $\nu_{\text{(Aryl-O)}}$ band by a value of +7 to -15 cm^{-1} . Meanwhile, subsequent to the process of complexation, it has been shown that the absorption bands associated with the azomethine and thiocarbonyl groups of the unbound FSATH have seen significant shifts towards lower wavenumbers, specifically by 20-35 and 18-49 cm^{-1} , respectively (refer to the experimental section for further details). The observed decrease in wavenumber values suggests that there is coordination between the imine-N of the Schiff base segment and the thiocarbonyl-S of the thiohydantoin ring with the metal ions [6,7]. The results of this study demonstrated that the FSATH ligand moiety coordinates through the azomethine nitrogen, phenolic oxygen, and thiocarbonyl sulfur atoms of the ligand. As a result, FSATH functions as a monoanionic (ONS) tridentate ligand.

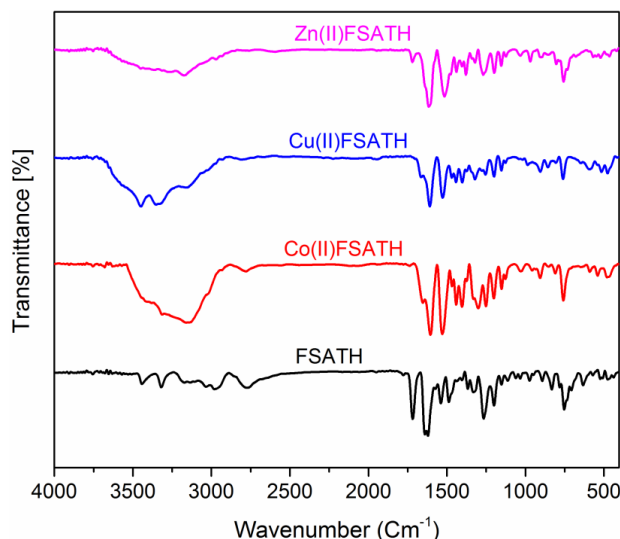


Figure 3: FTIR spectra of the parant (fluorosallycidene)-aminothiohydantoin ligand (FSATH) and its M(II)-coordination compounds for showing the changes in the characteristic peaks due to complexation.

3.2.3. UV-Vis spectra

DMSO solutions of FSATH and its M(II) coordination compounds at concentrations of 10^{-3} M were analyzed for their electronic absorption spectra. **Table 1** lists assignments for electronic spectral peaks characteristic of each compound. Three prominent absorption peaks stand out in the FSATH spectra. At

224 and 265 nm, the first two peaks were seen, and they were attributed to the $\pi \rightarrow \pi^*$ transition of the thiohydantoin and benzene rings. The emergence of the third peak occurred at around 349 nm, and this can be ascribed to the $n \rightarrow \pi^*$ transition that involves different electron-rich groups found in the ligand, such as C=O, C=N, and C=S. [11]. When the electronic spectra of coordination compounds are compared to those of the parent ligand (FSATH), a bathochromic shift and hypochromia of the major peaks could be observed, showing coordination of FSATH with M(II) ions. Specifically, the azomethine group's $n \rightarrow \pi^*$ band, originally at 349 nm, exhibited a significant shift and lost a lot of its intensity in the process. The obtained results provide support for the hypothesis that the observed alteration in the $n \rightarrow \pi^*$ transition is attributed to the presence of the azomethine group in the ligand, which coordinates with the metal ion [12]. For example, three distinct electronic transition bands ($\pi \rightarrow \pi^*$, $n \rightarrow \pi^*$) may be seen in the electronic spectrum of the Mn-FSATH complex at 233, 283, and 402 nm. The collective findings, in conjunction with the magnetic moment measurement of the Mn(II) complex (5.80 BM), provide compelling evidence supporting the presence of a high spin d^5 configuration in the Mn(II) ion. Furthermore, these results confirm the resulting paramagnetic behavior shown by the complex and the octahedral arrangement around the Mn(II) ion [7]. Similarly, in addition to the main characteristic ligand peaks (observed at 268 nm for $\pi \rightarrow \pi^*$ and 418 for $n \rightarrow \pi^*$) in the electronic spectrum of Co-FSATH, two new broad bands emerged at 521 and 681 nm which be assigned to the ${}^4T_{1g}(F) \rightarrow {}^4A_{2g}(F)(v_2)$ and ${}^4T_{1g}(F) \rightarrow {}^4T_{1g}(P)(v_3)$ transitions, respectively, in agreement with the cobalt(II) ion's octahedral coordination geometry [13]. Concurrently, the Co-FSATH complex's magnetic moment is 4.58 BM, which falls within the range previously documented for a high spin six-coordinated Co(II) complex with a d^7 configuration [13,14].

Table 1: FTIR and UV-Vis spectral peaks (λ_{\max} , nm) coupled with their assignments and the values of magnetic moments (BM) for the FSATH ligand and its coordination compounds

Sample	Vibrational band									Electronic transitions			μ_{eff} BM
	$\nu_{\text{(OH/NH)}}$	$\nu_{\text{(C=O)}}$	$\Delta\nu_{\text{(C=O)}}$	$\nu_{\text{(C=N)}}$	$\Delta\nu_{\text{(C=N)}}$	$\nu_{\text{(C=S)}}$	$\Delta\nu_{\text{(C=S)}}$	$\nu_{\text{(Ph-O)}}$	$\Delta\nu_{\text{(Ph-O)}}$	$\pi \rightarrow \pi^*$	$n \rightarrow \pi^*$	d \rightarrow d	
FSATH	3442	1716	–	1640	–	1488	–	1266		224, 265	349	–	–
Mn-FSATH	3430	1715	-1	1620	-20	1470	-18	1273	+7	233, 283	402	517	5.80
Co-FSATH	3432	1716	0	1605	-35	1467	-21	1251	-15	268	418	521, 681	4.58
Cu-FSATH	3338	1717	+1	1609	-31	1469	-19	1254	-12	264	374	579, 641	1.82
Zn-FSATH	3338	1715	-1	1615	-25	1439	-49	1258	-18	222, 263	319	–	–

Contrarily, the Cu-FSATH complex demonstrates hypsochromic shifts in the parent ligand's $\pi \rightarrow \pi^*$ and $n \rightarrow \pi^*$ transition peaks to a range of 233-402 nm in its electronic spectrum. Additionally, the spectrum displays relatively weak and broad peaks at 579 nm and 641 nm, which are indicative of the electronic transitions d \rightarrow d of type ${}^2B_{1g} + {}^2A_{1g}$ and ${}^2B_{1g} \rightarrow {}^2E_g$, respectively. Based on the obtained data, it has been postulated that the Cu-FSATH complex adopts a square planar geometry. Additionally, it was determined that the magnetic moment of the Cu(II) complex is 1.82 BM, which corresponds to the magnetic moment often attributed to square planar Cu(II) coordination compounds [7].

Since Zn(II) contains d-orbitals that are all filled to d^{10} , the Zn-FSATH complex is predicted to be diamagnetic and free of d \rightarrow d transitions. The Zn-FSATH complex shows solely absorption peaks at 222, 263, and 319 nm, which are displaced by -30 nm compared to the original ligand. These absorption bands arise from $\pi \rightarrow \pi^*$ and $n \rightarrow \pi^*$ transitions. Conclusions about the Zn(II) complex's square planar shape were

drawn from the results of the electronic spectrum [7,15] and thermal investigation (to be detailed below).

3.2.4. NMR spectroscopy

In this study, we examined the tautomeric equilibria existing between thiohydantoin thiol (T_{S-H}) and thione (T_{N-H}), as well as the relative distribution of tautomeric forms in deuterated solutions of the ligand (fluorosalicylidene)-aminothiohydantoin (FSATH). The comparison of the NMR spectral data of FSATH (see to **Figure 3** and the experimental section for additional information) with those of previously documented thiohydantoin derivatives [16,17] was conducted. The ^1H NMR spectrum of FSATH (**Figure 4**) exhibits three singlets at δ 11.40, 11.16, and 10.92 ppm. These signals are potentially associated with the phenolic O-H group of the salicylidene fragment and the thioamide N-H group characteristic of the T_{N-H} tautomer [18]. In contrast, the lack of an S-H singlet peak at around 4.5 ppm in the deuterated solution of the thiohydantoin ligand provided evidence that the T_{S-H} tautomer does not significantly contribute to the tautomeric equilibrium [18]. The SH/NH peak intensity ratio reveals that the thione form (T_{N-H}) of FSATH's core backbone accounts for 100% of the solution, with the thiol form (T_{S-H}) contributing 0%.

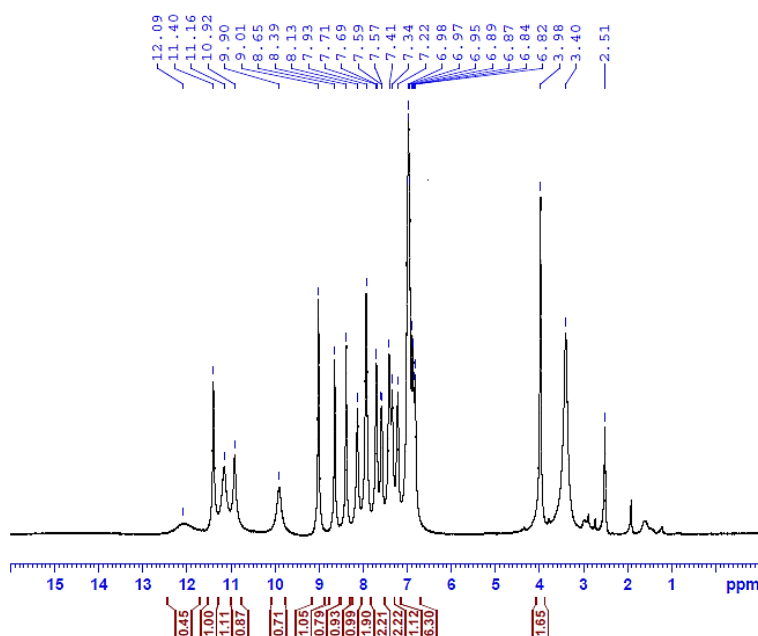


Figure 4: ^1H NMR of FSATH solution in $\text{DMSO-}d_6$ (200 MHz)

Additional proof that the FSATH's central backbone exists exclusively as thione (T_{N-H}) in its deuterated solution is provided by ^{13}C NMR spectroscopy. As per the findings of Kobyka et al., the ^{13}C resonance of the C-S peak exhibits a shift from 178 ppm in the case of a pure thione tautomer to 158 ppm in the case of a pure thiol tautomer [18]. In the ^{13}C NMR spectra of thiohydantoin ligands (**Figure 5**), there are four distinct signals observed at chemical shift values of approximately 178, 174, 165, and 163 ppm. These signals can be attributed to the resonance of carbon atoms belonging to the thiocarbonyl (C=S), carbonyl (C=O), and azomethine (HC=N) functional groups, respectively. It is worth noting that the absence of any peak observed at around 158 indicates that the T_{S-H} tautomeric form does not participate in the molecular structure of the thiohydantoin ligand solution.

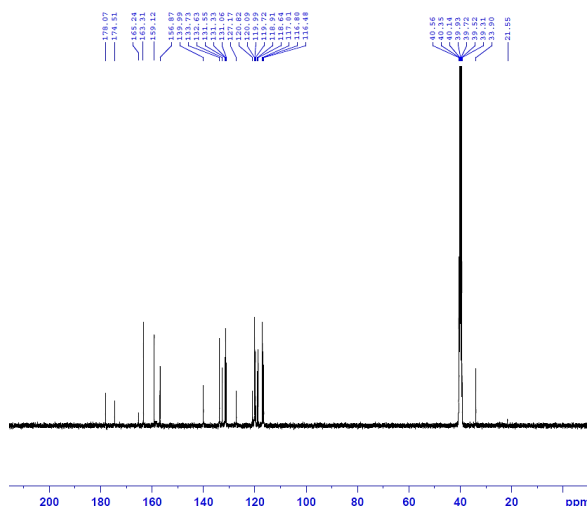
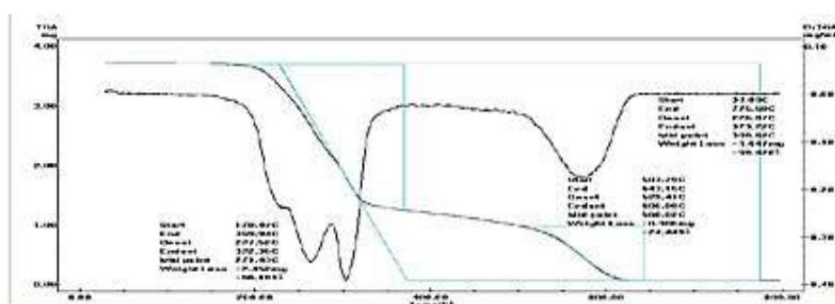


Figure 5: ¹³C NMR of FSATH solution in DMSO-d₆ (100 MHz)

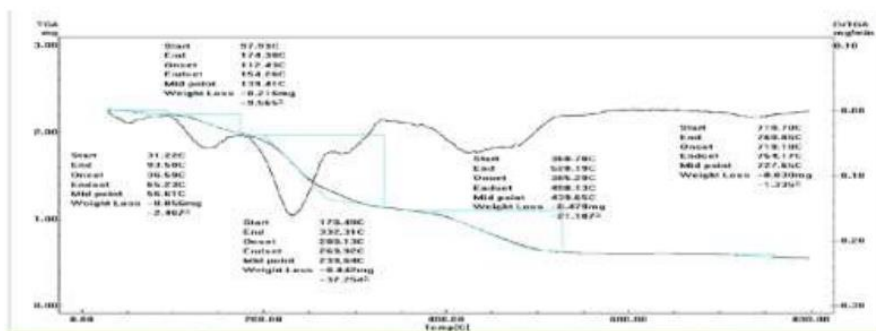
3.2.5. Thermal analysis

Thermogravimetric analysis (TGA) and differential thermogravimetric analysis (DTG) are powerful techniques used in the field of chemistry to study the thermal behavior of materials. Therefore, TGA and DTG were applied to examine the thermal behavior of the ligand and its coordination compounds. The TGA results showed that the FSATH ligand is thermally stable up to 227.52 °C and exhibited a two-step decomposition process, with a total weight loss of 98.43 % at a temperature of 606.08 °C. On the other hand, the coordination compounds displayed multi-step decomposition processes, indicating the presence of multiple components within the coordination compounds. The DTG analysis further revealed that the ligand and its coordination compounds exhibited different decomposition temperatures and decomposition rates. The coordination compounds displayed multiple peaks at different temperatures, indicating the presence of different components with varying thermal stabilities. These findings suggest that the formation of coordination compounds with the ligand alters its thermal behavior and stability. Additionally, the study also demonstrated that the ligand and its coordination compounds exhibited different weight loss patterns, indicating the presence of different types of bonds and interactions within the coordination compounds.



Start	170.47 C	583.79 C	33.09 C
End	369.94 C	643.15 C	775.68 C
Onset	227.52 C	529.41 C	226.87 C
Endset	322.36 C	606.08 C	373.22 C
Mid Point	271.43 C	568.62 C	308.22 C
Weight Less	-2.452 mg	-8.906 mg	-3.647 mg
	-66.101%	-24.449 %	-98.428 %

Figure 6: TGA and DTG curves of FSATH ligand



Start	31.22 C	97.93 C	178.49 C	360.70 C	710.70 C
End	93.50 C	174.38 C	332.31 C	528.19 C	760.86 C
Onset	36.59 C	112.43 C	200.13 C	385.29 C	718.18 C
Endset	65.23 C	154.26 C	269.92 C	490.13 C	754.17 C
Mid Point	56.61	139.41 C	239.64 C	439.65 C	727.65 C
Weight Less	-0.056 mg	-0.216 mg	-0.842 mg	-0.479 mg	-0.030 mg
	-2.467%	-9.565 %	-37.254 %	-21.1 87 %	-1.335 %

Figure 7: TGA and DTG curves of Mn-FSATH complex

3.3. Anticancer activity

The main objective of this study is to develop metal(II) thiohydantoin Schiff base coordination compounds that are both safe and cytotoxic, with the intention of utilizing them in the treatment of breast cancer. In order to achieve this objective, the new ligand (FSATH) and its corresponding metal coordination compounds (M-FSATH) were subjected to *in vitro* evaluation for their potential anticancer activity against breast carcinoma cell lines (MCF-7). The results were then compared with those obtained from a clinical anticancer drug, 5-fluorouracil (5-FU).

3.3.1. MTT assay

Figure 8 shows that all of the compounds inhibited the proliferation of carcinoma cells (MCF-7) in culture, with the effectiveness depending on the treatment agent's structural properties and the concentration of the samples. It is worth noting that the M-FSATH coordination compounds exhibited more pronounced inhibitory anticancer effects compared to those caused by the free FSATH ligand. This is because the chelation of metal ions causes the entire molecule to become more planar, the metallacycle forms a more extensive electron delocalization system (Figure 9), and there are more electrostatic interactions inherent to the molecule because of the metal ion's presence [19]. The sequence of efficacy patterns was as follows: the inhibitory concentration (IC_{50}) values for various compounds were determined as follows: Cu-FSATH exhibited the highest potency with an IC_{50} of $6.02 \pm 0.30 \mu\text{g/mL}$, followed by Zn-FSATH with an IC_{50} of $9.72 \pm 0.52 \mu\text{g/mL}$. Comparatively, 5-FU demonstrated a lower potency with an IC_{50} of $17.92 \pm 0.95 \mu\text{g/mL}$. Mn-FSATH exhibited a higher IC_{50} value of $22.81 \pm 1.29 \mu\text{g/mL}$, while Co-FSATH demonstrated an even higher IC_{50} value of $38.34 \pm 2.17 \mu\text{g/mL}$. Finally, FSATH exhibited the lowest potency among the compounds tested, with an IC_{50} of $65.13 \pm 2.66 \mu\text{g/mL}$.

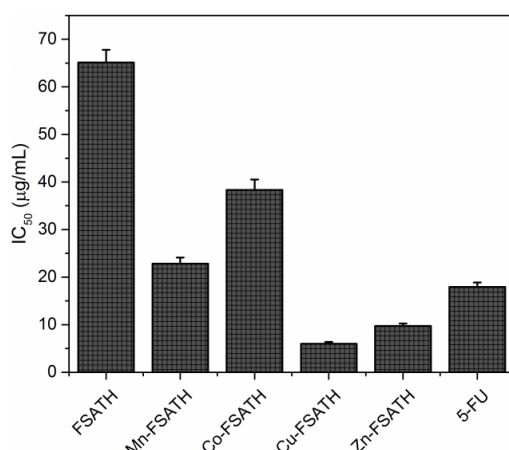


Figure 8: The IC₅₀ values (µg/ mL) of the new ligand (FSATH) and its corresponding metal coordination compounds (M-FSATH) against MCF-7 cancer cells

Notable, metal complex planarity plays a crucial role in the interaction between metal coordination compounds and DNA, ultimately impacting DNA damage. The planar metal coordination compounds tend to intercalate between the DNA base pairs, leading to disruption of the double helical structure and interfering with DNA replication and transcription processes. This intercalation mode of binding is facilitated by the flat coordination geometry of the metal complex, which allows for optimal π - π stacking interactions with the DNA bases. Furthermore, the planarity of metal coordination compounds also influences their cytotoxicity. Sathyadevi et al. explain that planar metal coordination compounds possess higher cytotoxicity compared to non-planar coordination compounds. This can be attributed to their enhanced ability to interact with DNA and induce DNA damage, leading to cell death. The planarity of metal coordination compounds thus plays a crucial role in their DNA binding and cytotoxicity, highlighting the importance of understanding and controlling the structural features of these coordination compounds in the design of potential therapeutic agents [20].

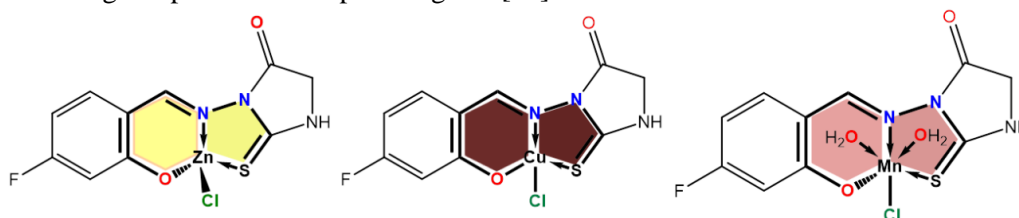


Figure 9: Structural features of the new M-FSATH coordination compounds showing the five-membered and six-membered metallocyclic rings.

The superior efficacy of the Cu(II) complex, compared to the free ligand and other coordination compounds, could be attributed to their ability to induce oxidative stress and disrupt mitochondrial function in cancer cells. Additionally, the interaction of the Cu(II) coordination compounds with DNA was found to play a crucial role in their anticancer activity. The Cu(II) coordination compounds were shown to effectively bind to DNA, leading to DNA damage and subsequent cell death. Furthermore, the coordination compounds were found to inhibit the activity of topoisomerase II, an enzyme involved in DNA replication and repair. These findings highlight the multifaceted mechanisms behind the superior efficacy of Cu(II) coordination compounds against MCF-7 cells and provide valuable insights for the development of novel anticancer agents [22].

4. CONCLUSION

This study presents a facile protocol for preparing a new ligand, (fluorosalicylidene)-aminothiohydantoin (FSATH), using 4-fluorosalicylaldehyde as a starting substrate. Consequently, this

ligand reacted with various metal(II) chlorides in a stoichiometric ratio of 1:1 to obtain the corresponding coordination compounds containing Mn(II), Co(II), Cu(II), and Zn(II) ions. Through the application of diverse physicochemical and spectroscopic techniques (FTIR, UV-Vis, NMR, and EI-MS), the structural characteristics as well as coordination modes of FSATH with M(II) ions were investigated. Additionally, the TGA and DTA techniques have been employed to confirm the thermal stability of new compounds. The results of the cytotoxicity assay demonstrated that all coordination compounds are more potent against breast cancer cell lines (MCF-7) as compared to the parent ligand. These findings suggest that these coordination compounds have the potential to be considered as promising candidates for the development and investigation of novel chemotherapeutic agents in the field of cancer therapy, as demonstrated by the comparative in-vitro anticancer studies conducted. Cu-FSATH demonstrates significant cytotoxicity against MCF-7, making it a highly promising candidate as an alternative to conventional chemotherapeutic agents

5. REFERENCES

- [1] S. Zhang *et al.*, "Efficient drug discovery by rational lead hybridization based on crystallographic overlay," *Drug Discov Today*, vol. 24, no. 3, pp. 805–813, Mar. 2019, doi: 10.1016/j.drudis.2018.11.021.
- [2] V. Abbot, P. Sharma, S. Dhiman, M. N. Noolvi, H. M. Patel, and V. Bhardwaj, "Small hybrid heteroaromatics: Resourceful biological tools in cancer research," *RSC Adv*, vol. 7, no. 45, pp. 28313–28349, 2017, doi: 10.1039/C6RA24662A.
- [3] S. H. Cho, S. H. Kim, and D. Shin, "Recent applications of hydantoin and thiohydantoin in medicinal chemistry," *Eur J Med Chem*, vol. 164, pp. 517–545, Feb. 2019, doi: 10.1016/j.ejmech.2018.12.066.
- [4] L. S. Akree, Z. A. Amin, and H. O. Ahmad, "In silico and in vivo hepatoprotective activity of the synthesized 5-benzylidene-2-thiohydantoin against diethylnitrosamine-induced liver injury in a rat model," *Sci Rep*, vol. 13, no. 1, Dec. 2023, doi: 10.1038/s41598-023-27725-x.
- [5] O. A. Abu Ali *et al.*, "New Mn(III)/Fe(III) complexes with thiohydantoin-supported imidazolium ionic liquids for breast cancer therapy," *Inorganica Chim Acta*, vol. 551, Jun. 2023, doi: 10.1016/j.ica.2023.121460.
- [6] L. A. Ismail *et al.*, "Novel imidazolium-thiohydantoin hybrids and their Mn(iii) complexes for antimicrobial and anti-liver cancer applications," *RSC Adv*, vol. 12, no. 44, pp. 28364–28375, Oct. 2022, doi: 10.1039/d2ra05233d.
- [7] A. R. E. Mahdy, M. Y. Alfaifi, M. S. El-Gareb, N. Farouk, and R. F. M. Elshaarawy, "Design, synthesis, and physicochemical characterization of new aminothiohydantoin Schiff base complexes for cancer chemotherapy," *Inorganica Chim Acta*, vol. 526, Oct. 2021, doi: 10.1016/j.ica.2021.120504.
- [8] M. M. Elbadawi, A. I. Khodair, M. K. Awad, S. E. Kassab, M. T. Elsaady, and K. R. A. Abdellatif, "Design, synthesis and biological evaluation of novel thiohydantoin derivatives as antiproliferative agents: A combined experimental and theoretical assessments," *J Mol Struct*, vol. 1249, p. 131574, Feb. 2022, doi: 10.1016/j.molstruc.2021.131574.
- [9] R. F. M. Elshaarawy, Y. Lan, and C. Janiak, "Oligonuclear homo- and mixed-valence manganese complexes based on thiophene- or aryl-carboxylate ligation: Synthesis, characterization and magnetic studies," *Inorganica Chim Acta*, vol. 401, pp. 85–94, May 2013, doi: 10.1016/j.ica.2013.03.019.
- [10] Y. A. Hassan, A. I. M. Khedr, J. Alkabli, R. F. M. Elshaarawy, and A. M. Nasr, "Co-delivery of imidazolium Zn(II)salen and Origanum Syriacum essential oil by shrimp chitosan nanoparticles for antimicrobial applications," *Carbohydr Polym*, vol. 260, May 2021, doi: 10.1016/j.carbpol.2021.117834.

- [11] V. Deval *et al.*, “Molecular structure (monomeric and dimeric) and hydrogen bonds in 5-benzyl 2-thiohydantoin studied by FT-IR and FT-Raman spectroscopy and DFT calculations,” *Spectrochim Acta A Mol Biomol Spectrosc*, vol. 132, pp. 15–26, Nov. 2014, doi: 10.1016/j.saa.2014.04.101.
- [12] Y. A. Hassan, M. Y. Alfaifi, A. A. Shati, S. E. I. Elbehairi, R. F. M. Elshaarawy, and I. Kamal, “Co-delivery of anticancer drugs via poly(ionic crosslinked chitosan-palladium) nanocapsules: Targeting more effective and sustainable cancer therapy,” *J Drug Deliv Sci Technol*, vol. 69, Mar. 2022, doi: 10.1016/j.jddst.2022.103151.
- [13] S. S. Kandil, G. B. El-Hefnawy, E. A. Bakr, and A. Z. Abou El-Ezz, “Cobalt(II), nickel(II) and copper(II) complexes of 5-(2-carboxyphenylazo)-2-thiohydantoin,” *Transition Metal Chemistry*, vol. 28, no. 2, pp. 168–175, Mar. 2003, doi: 10.1023/A:1022968604281/METRICS.
- [14] A. B. P. Lever and S. A. Rice, “Inorganic Electronic Spectroscopy,” *Phys Today*, vol. 22, no. 10, pp. 77–77, Oct. 1969, doi: 10.1063/1.3035225.
- [15] K. R. Balinge, A. G. Khiratkar, P. N. Muskawar, K. Thenmozhi, and P. R. Bhagat, “Facile access to polymer supported zinc–salen complex: highly efficient heterogeneous catalyst for synthesizing hydantoins, thiohydantoins and Schiff bases in aqueous medium,” *Research on Chemical Intermediates*, vol. 44, no. 3, pp. 2075–2097, Mar. 2018, doi: 10.1007/s11164-017-3215-x.
- [16] B. V. Trzhtsinskaya and N. D. Abramova, “Imidazole-2-Thiones: Synthesis, Structure, Properties,” *Sulfur reports*, vol. 10, no. 4, pp. 389–421, Jun. 1991, doi: 10.1080/01961779108048760.
- [17] E. G. Jayasree and S. Sreedevi, “A DFT study on protic solvent assisted tautomerization of heterocyclic thiocarbonyls,” *Chem Phys*, vol. 530, p. 110650, Feb. 2020, doi: 10.1016/j.chemphys.2019.110650.
- [18] K. Kobyłka, G. Żuchowski, W. Tejchman, and K. K. Zborowski, “Synthesis, spectroscopy, and theoretical calculations of some 2-thiohydantoin derivatives as possible new fungicides,” *J Mol Model*, vol. 25, no. 9, Sep. 2019, doi: 10.1007/s00894-019-4146-9.
- [19] B. Mendiguchia, I. Aiello, A. C.-D. Transactions, and undefined 2015, “Zn (II) and Cu (II) complexes containing bioactive O, O-chelated ligands: homoleptic and heteroleptic metal-based biomolecules,” *pubs.rsc.orgBS Mendiguchia, I Aiello, A CrispiniDalton Transactions, 2015•pubs.rsc.org*, vol. 00, pp. 1–3, 2013, doi: 10.1039/x0xx00000xReceived.
- [20] P. Sathyadevi, P. Krishnamoorthy, R. R. Butorac, A. H. Cowley, N. S. P. Bhuvanesh, and N. Dharmaraj, “Effect of substitution and planarity of the ligand on DNA/BSA interaction, free radical scavenging and cytotoxicity of diamagnetic Ni(ii) complexes: A systematic investigation,” *Dalton Transactions*, vol. 40, no. 38, pp. 9690–9702, Oct. 2011, doi: 10.1039/c1dt10767d.